RSC Advances

PAPER

View Article Online
View Journal | View Issue

Cite this: *RSC Adv.*, 2021, **11**, 14624

One-pot green synthesis of gold and silver nanoparticles using *Rosa canina* L. extract†

Pablo Eduardo Cardoso-Avila,[a] Rita Patakfalvi,*[b] Carlos Rodríguez-Pedroza,[b] Xochitl Aparicio-Fernández,[b] Sofía Loza-Cornejo,[b] Virginia Villa-Cruz[b] and Evelia Martínez-Cano[b]

Received 23rd February 2021
Accepted 10th April 2021

DOI: 10.1039/d1ra01448j

rsc.li/rsc-advances

This study reports a green, simple, and fast method for the synthesis of gold and silver nanoparticles using natural antioxidant compounds. The aqueous extract from dried rosehips (pseudofruit of *Rosa canina* L.) was used as a reducing and capping agent of $HAuCl_4$ and $AgNO_3$ during the noble metal colloid synthesis at room temperature and no other chemical reagent was used. The high antioxidant activity of the plant extract was proven by 2,2-diphenyl-1-picrylhydrazyl assay by a spectrophotometric method. The formation of stable gold and silver nanoparticles was observed by UV-visible spectroscopy and the evolution of their characteristic surface plasmon resonance band was followed over several days. Transmission electron microscopy confirmed the formation of quasi-spherical nanoparticles with mean diameters 26 and 34 nm, for gold and silver nanoparticles, respectively; XRD revealed an FCC crystalline structure for both gold and silver NPs. The effects of concentrations of noble metal precursor and plant extract solution on the formation, stabilization and size of nanoparticles are discussed, as well as some applications of these colloids.

Introduction

Noble metal nanoparticles (NPs) are one of the most investigated aspects of nanoscale materials due to their extraordinary chemical, physical, optical, and electronic properties.[1–3] Owing to these properties, these nanomaterials have many applications in different fields, such as in medicine, biology, catalysis, electronics, and photonics, among others.[1,4–8]

There are different physical, chemical, and biological methods for synthesizing noble metal nanoparticles, however the most commonly applied are the ones based on chemical reduction. Subsequent to the classic Turkevich method,[9] many types of synthesis protocols have been published in the literature,[1–5] however, most of these methods involve hazardous chemicals or residues. Green and biological methods offer an alternative way of eliminating or minimizing the use of environmental-risk materials.[10–18] These syntheses involve biological systems such as bacteria, fungus, and plants; however, the use of plant extracts is the most popular method because is the simplest extracellular syntheses for obtaining metallic nanoparticles on a large scale. A great variety of plants extracts have been used to synthesize metallic nanoparticles. Different secondary metabolites, for example alkaloids, flavonoids, saponins, steroids, tannins, terpenoids, polyphenols, phenolic acids, ketones, aldehydes, as well as polysaccharides, amino acids, proteins and vitamins present in plant extracts, are involved in the reduction of metal cations and the stabilization of the nanoparticles formed.[10–18] Generally, natural antioxidants are able to reduce silver and gold cations and some previous works have used this property to assess the antioxidant potential of different phytochemicals.[19–21]

In particular, rosehip, the pseudofruit of *Rosa canina* L., is well-known for its excellent antioxidant properties.[22] Previous studies confirmed that rosehip extracts contain active compounds such as ascorbic acid, carotenoids, phenolic compounds (phenolic acids; flavonoids like proanthocyanidin), polyunsaturated fatty acids and phospholipids, among others.[23–26] These compounds should act as reducing and/or stabilizing agents during metallic nanoparticle synthesis. *Rosa canina* extracts have been used successfully for the green synthesis of palladium,[27] gold[28,29] and silver[28,30] nanoparticles, as well as oxide nanoparticles like zinc oxide[31] and copper oxide[32] nanoparticles. Moreover, this plant extract also allowed the green synthesis of hybrid organometallic nanomaterials like palladium nanoparticles supported on graphene oxide.[33,34] All these synthesis methods used other reactants or pH adjusting and were carried at temperatures ranging from 60 to 100 °C. Pulit and Banach investigated the effect of metal salt concentration, reaction pH and temperature to the nanoparticle formation.[28] The smallest nanoparticles (silver with 47.44 nm

[a]*Centro de Investigaciones en Óptica, A.C., Loma del Bosque 115, 37150, León, Guanajuato, Mexico*

[b]*Centro Universitario de los Lagos, Universidad de Guadalajara, Enrique Díaz de León 1144, 47463, Lagos de Moreno, Jalisco, Mexico. E-mail: rpatakfalvi@culagos.udg.mx*

† Electronic supplementary information (ESI) available. See DOI: 10.1039/d1ra01448j

and gold with 17.24 nm average size) were synthesized at pH 12. Khademi-Azandehi *et al.* published the synthesis of gold nanoparticles with anti-HIV characteristics.[29] They described one method using 85 °C reaction temperature and gold NPs with 27.7 nm average size were obtained. The same temperature was applied to prepare silver nanoparticles.[30] TEM measurements showed that the particle size was 13–21 nm. The synthesized NPs were found to be highly effective for antioxidant, antibacterial, antifungal, and DNA cleavage activities.

Here, we present a one-pot green, simple and fast method for the synthesis of gold and silver nanoparticles using natural antioxidant compounds. Aqueous extract from dried rosehips (pseudofruit of *Rosa canina* L.) was used as a reducing and capping agent of $HAuCl_4$ and $AgNO_3$ during the noble metal colloid synthesis at room temperature and no other chemical reagent was used. The formation of stable gold and silver nanoparticles was observed by UV-visible spectroscopy and the evolution of their characteristic surface plasmon resonance band was followed over several days. The effect of concentrations of noble metal precursor and plant extract solution on the formation, stabilization and size of nanoparticles are discussed. Transmission electron microscopy confirmed the formation of quasi-spherical nanoparticles and some applications of these colloids are presented.

Materials and methods

During the experiments, the following materials were used as received: silver nitrate ($AgNO_3$, Sigma Aldrich, 99.9%), gold(III) chloride trihydrate ($HAuCl_4$, Sigma Aldrich, 99.9%), 2,2-diphenyl-1-picrylhydrazyl (DPPH, Sigma-Aldrich, 99%) and dried rosehip of *Rosa canina* L. (Rosae pseudo-fructus, Naturland, Hungary). All glassware was cleaned with aqua regia and thoroughly rinsed with deionized water before being used.

Preparation of *Rosa canina* L. extract

For the *Rosa canina* L. extract preparation, 100 mL of deionized water were heated to boil, then 2 g of Rosae pseudo-fructus were added and boiling continued for 10 minutes. The preparation was left to cool until room temperature, decanted and gauged to 100 mL with deionized water to compensate the volume lost due to evaporation. This extract, used as a stock solution, was reserved at 4 °C in a light covered recipient and used in no more than two days after preparation. Four dilutions of the plant extract were also prepared using deionized water (20, 40, 60 and 80% vol/vol); these dilutions, and the non-diluted stock plant extract, were used as reductants in the synthesis of gold and silver nanoparticles.

Synthesis of gold and silver nanoparticles

Gold and silver nanoparticles were prepared using two different $HAuCl_4$ and $AgNO_3$ concentrations, 1×10^{-2} and 1×10^{-3} M. The synthesis method was the same for the gold and silver nanoparticles: the metallic salt solutions (5 mL) were placed in a beaker under vigorous magnetic stirring and 5 mL of the diluted plant extract solutions were fast injected. Once the plant extract was added to the metallic salt a change in coloration was visible to the eye indicating the formation of noble metal nanoparticles. The mixture was left to react for 15 minutes and then reserved. Table 1 includes the details on the preparation and the labels assigned to each sample.

Table 1 Details on the preparations of the gold and silver colloids and sample label assignation

Dilution of stock plant extract [% vol/vol]	$HAuCl_4$ concentration (M)		$AgNO_3$ concentration (M)	
	1×10^{-2}	1×10^{-3}	1×10^{-2}	1×10^{-3}
20	G20-2	G20-3	S20-2	S20-3
40	G40-2	G40-3	S40-2	S40-3
60	G60-2	G60-3	S60-2	S60-3
80	G80-2	G80-3	S80-2	S80-3
100	G100-2	G100-3	S100-2	S100-3

Characterization

UV-visible extinction spectra of plant extract and synthesized gold and silver nanoparticles were collected in a Cary 60 spectrophotometer over a spectral range from 200 to 800 nm, using a 1 cm quartz cuvette. One droplet of the colloidal solutions was deposited onto a carbon coated copper grid and allowed to dry at room temperature. High-resolution transmission electron micrographs (HRTEM) were obtained using a FEI TECNAI F30 microscope, operated at 300 kV. Scanning electronic microscopy (SEM) was performed using a JSM-7800F JEOL (Tokyo, Japan) microscope: a 2 μL drop of each sample was placed on top of an aluminized glass substrate and allowed to dry at room temperature. All the SEM images were obtained using a 15 kV accelerating voltage. The nanoparticles size distribution was determined by using ImageJ software, a minimum of 200 particles were measured. Fourier transform infra-red (FTIR) spectra from 4000 to 900 cm^{-1} were acquired using a Cary 670 FTIR coupled to a Cary 620 FTIR spectrometer (Agilent Technologies, USA) and equipped with an attenuated total reflection module (ATR). 25 μL drops of the gold and silver colloids were allowed to dry at room temperature on top a of clean glass substrate; once dried, subsequent drops were placed on the same spots in order to increase the NPs concentration. The drying process was repeated 9 times. After the FTIR analysis, the gold and silver NPs powders were scraped from the glass substrates and X-ray diffractograms were obtained using an XRD D2 Phaser Bruker equipment, with a Bragg–Brentano geometry and Cu-kα radiation ($\lambda = 1.5418$ Å). Surface Z-potentials of diluted gold nanoparticles (GNPs) and silver nanoparticles (SNPs) were measured using a Malvern Zetasizer Nano ZS apparatus.

Results and discussion

Characterization of *Rosa canina* L. extract

Rosa canina L. extract was used as a reducing agent in the preparation of colloidal gold and silver. To reveal the antioxidant capacity of the plant extract, the free radical scavenging activity of *Rosa canina* L. extract was measured spectrophotometrically using the DPPH assay[35,36] (see ESI, Fig. S1†). The elevated antiradical activity obtained suggests that this extract is a good reductive agent for gold and silver cations.[37]

The UV-Vis absorbance spectrum of plant extract was also analysed to exclude interference with the spectrum of DPPH and the noble metal nanoparticles (Fig. S1†). There is an absorbance band at 280 nm, but there is no notable absorbance in the gold (500–600 nm) and silver (380–420 nm) nanoparticles surface plasmon band ranges. Phytochemical characterization of this extract reported in previous publications observed that ascorbic acid concentration is lower in dried rosehips and suggest that antioxidant properties are mainly the result of high phenolic concentration.[24,26]

Synthesis and characterization of gold and silver nanoparticles

Gold nanoparticles were analysed by UV-visible spectroscopy, which detects the evolution of their characteristic surface plasmon resonance band during synthesis.[38] The colour of aqueous $HAuCl_4$ solution changed immediately after the addition of *Rosa canina* L. extract, indicating the formation of gold nanoparticles and that the extract acted as a reducing agent for gold cations. In the case of the GNPs synthesized using $HAuCl_4$ 1×10^{-2} M solution, as the concentration of the plant extract in the reaction was increased, the extinction value of the plasmon band was higher (see Fig. 1A and C).

The GNPs UV-Vis spectra were monitored for seven days after the synthesis. Small spectral differences were perceived during the first 4 days, but after 5 days no more changes occurred, indicating that the reaction finished, and the GNPs stabilized. The UV-Vis spectra collected on day 1 for samples G20-2 and G40-2, the two samples synthesized with the more diluted extracts, showed an absorption band associated to $HAuCl_4$ at 310 nm after the reduction process. This band was also detected in the spectrum of sample G20-2 after 5 days, but it was not present in the spectrum collected of sample G40-2; this implies that the reducing agent was not sufficient to reduce all of the gold cations in the mixture for both samples. To obtain information about the reaction yield we compared the absorbance values of each samples at 400 nm (Abs_{400}). According to Hendel *et al.* the Abs_{400} can scale linearly with the Au(0) concentration in gold nanoparticle solutions and enable its direct determination.[39] Without knowing the extinction coefficients of our solutions, we only compared the gold concentrations of the different samples. Abs_{400} as function of extract dilution is shown in ESI, Fig. S2.† Up to 80% of extract dilution, there is a linear increment in Abs_{400} values. Whereas with the maximum amount of extract (sample G100-2), the growth of Abs_{400} decreases. This result confirms that the added extract volume was not sufficient to reduce all the gold ions in the case of the first four samples, probably only for the G100-2 sample. Au(0) concentration is increasing linearly up to G80-2, then there is a smaller increment for G100-2. This behaviour could be the indication that total reduction has been achieved for this sample.

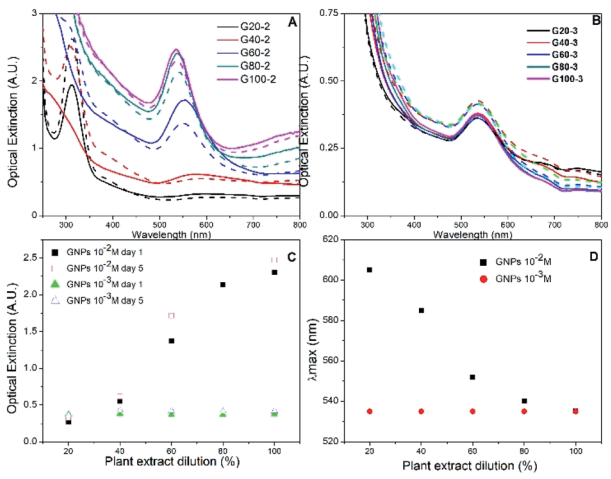

Fig. 1 UV-Vis absorption spectra of GNPs synthesized with different extract dilutions for $HAuCl_4$ concentration of 1×10^{-2} M (panel A) and 1×10^{-3} M (panel B), collected on day 1 (dashed lines) and day 5 (continuous lines). The maximum optical extinction and the plasmon band location as function of extract dilution are shown in panels (C) and (D) respectively.

Rosa canina L. extract was confirmed as also playing the role of stabilizing agent for the GNPs. When extract concentration was increased the plasmon resonance band shifted towards smaller wavelengths (Fig. 1D): utilizing 20% diluted plant extract (sample G20-2), the maximum absorbance value was located at 605 nm, whereas utilizing non diluted extract (sample G100-2), the plasmon band was located at 535 nm. This blue shift usually means a decrease in particle size.[40,41] Regarding the two samples with less extract (G20-2 and G40-2), precipitated particles were observed after one day. However, the other GNPs synthesized remained stable for more than one week and the absorption band was narrow, indicating the presence of uniform quasi-spherical gold nanoparticles.[40]

The dual role of the *Rosa canina* L. extract in nanoparticle synthesis (reducing and stabilizing agent) was also confirmed by synthesizing a set of GNPs using a lower $HAuCl_4$ concentration (1×10^{-3} M). Fig. 1B shows the UV-Vis spectra of gold colloids synthesized with different extract dilutions on the 1st and 5th days of preparation. Due to the formation of fewer nanoparticles, the absorbance values were lower than in the case of 1×10^{-2} M $HAuCl_4$ (Fig. 2A). Besides, the five samples showed similar plasmon bands and there was no significant difference between the Abs_{400} values (see Fig. S2†). This indicates that the amount of *Rosa canina* L. extract was sufficient to reduce all the Au^{3+} cations and stabilize the gold nanoparticle in all the samples. This stability was maintained for one week in the case of all five samples and only a small increase in the absorbance band was observed (Fig. 1C).

Particle size and morphology of GNPs of samples G100-2 and G100-3, the samples synthesized using the non-diluted *Rosa canina* L. extract, were acquired by transmission and scanning electron microscopy (TEM and SEM, respectively). The micrographs (Fig. 2A, B, and ESI Fig. S3A, B†) confirmed the formation of dispersed quasi-spherical metallic nanoparticles for both samples, and the average sizes were also similar for both $HAuCl_4$ concentrations: 27 ± 5 (1×10^{-2} M) and 26 ± 4 nm (1×10^{-3} M). Additionally, it is important to note that for the lowest gold concentration the size dispersity was lower (see Fig. S4 in ESI†). These size values agree with the UV-Vis spectroscopy data, which verifies, once again, our hypothesis that *Rosa canina* L.

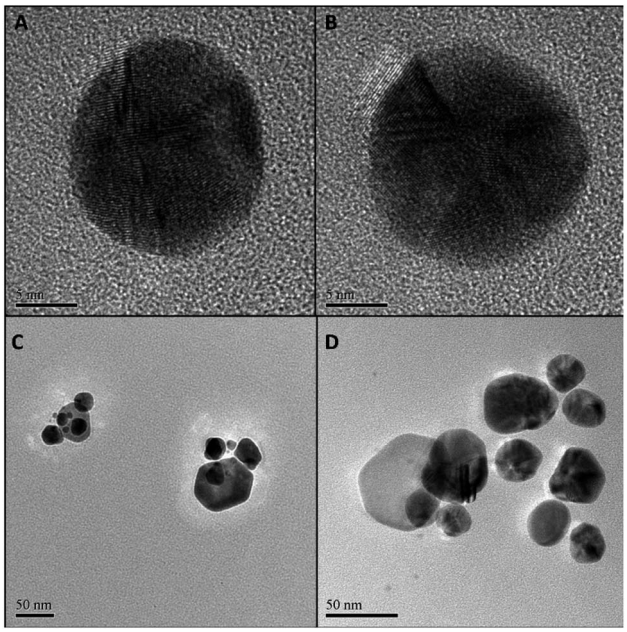

Fig. 2 TEM micrographs of samples G100-2 (panel A), G100-3 (B), S100-2 (C) and S100-3 (D).

extract plays a dual role in gold colloid synthesis as reducing and capping agent.

Since most reductants of $HAuCl_4$ can also be applied to $AgNO_3$, we wanted to probe if *Rosa canina* L. extract could also produce stable SNPs. The synthesis protocol was the same as in the case of the GNPs and UV-Vis spectroscopy was used to follow the SNPs formation. After the addition of *Rosa canina* L. extract, the $AgNO_3$ solution rapidly changed to a yellow-brownish colour indicating the formation of silver nanoparticles. Fig. 3A, shows the spectra recorded for a set of samples synthesized using an $AgNO_3$ 1×10^{-2} M solution and different plant extract dilutions. The spectra recorded the first day revealed a principal plasmon band located around 440 nm for all samples and a small shoulder around 580 nm for some of them. Moreover, likewise in the case of GNPs synthesis, the extinction value of the plasmon band increased as the plan extract was more concentrated, indicating the formation of more SNPs. Five days after the synthesis the reaction stabilized; no more spectral changes were perceived after this day. The extinction values for the 440 nm plasmon band increased considerably (Fig. 3C) and samples S100-2, S80-2 and S60-2 presented a second plasmon band around 580 nm. This second plasmon band is often attributed to the presence of anisotropic nanoparticles in the sol; this was confirmed by the TEM and SEM microscopies of sample S100-2 (Fig. 2C and S3C†), where a combination of quasi-spherical (34 ± 6 nm) and flat SNPs was detected. Furthermore, the principal band presented a small blue shift for most of the samples (Fig. 3D); the longest shift (8 nm) was for the S20-2, the sample prepared with the more diluted extract.

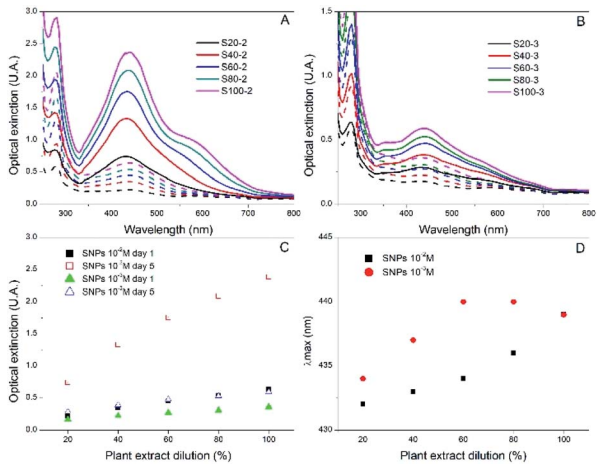

Fig. 3 UV-Vis absorption spectra of SNPs synthesized with different extract dilutions for $AgNO_3$ concentrations of 1×10^{-2} M (panel A) and 1×10^{-3} M (panel B), collected on day 1 (dashed lines) and day 5 (continuous lines). The maximum optical extinction and the plasmon band location on day 5 as function of extract dilution are shown in panels (C) and (D) respectively.

Given that *Rosa canina* L. extract was confirmed as an appropriate reducing and stabilizing agent for the synthesis of SNPs, a second set of samples was prepared using a lower $AgNO_3$ concentration (1×10^{-3} M). The extinction values were lower than the ones of the 1×10^{-2} M SNPs, indicating the formation of fewer SNPs (Fig. 3B). Contrary to occurred in the set of GNPs 1×10^{-3} M, in this set of SNPs the extinction values did increase as the reaction stabilized, for instance, sample S100-3 extinction augmented from 0.359 on day 1 to 0.591 on day 5 (Fig. 3C). The final plasmon bands were in the same range for both silver concentrations (Fig. 3D). Microscopy analysis performed to the sample S100-3 revealed a mean size of 33 ± 5 nm for the quasi-spherical SNPs and the presence of a few flat and twin nanoparticles (Fig. 2D and S3D†).

The crystalline structure of nanoparticles was studied by XRD analysis (Fig. 4). X-ray diffractograms of GNPs show four peaks at 38.2, 44.4, 64.6 and 77.6° which correspond to the (111), (200), (220) and (311) planes, respectively. This indicates a face centered cubic structure for the synthesized GNPs.[15] XRD patterns of SNPs showed peaks at 38.2, 44.3 and 77.7° corresponding to (111), (200) and (311) planes of face centered cubic silver.[42] The other peaks at 27.9, 32.25, 46.3 and 56.2° could be related to crystalline and amorphous organic phases as Kumar *et al.* identified in a previous work.[43]

FTIR spectroscopy was used to identify which plant extract molecules could be responsible in the metallic nanoparticle formation. Fig. 5 shows the FTIR spectrum of plant extract and spectra of the synthesized GNPs and SNPs. Similar results were

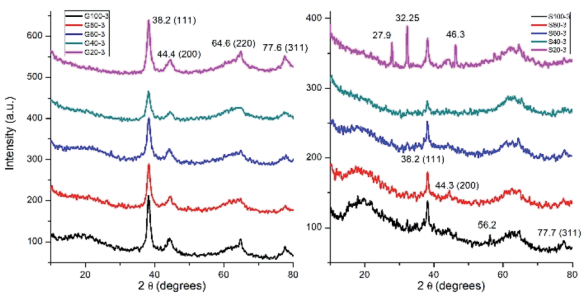

Fig. 4 X-ray diffraction analysis of GNPS and SNPs.

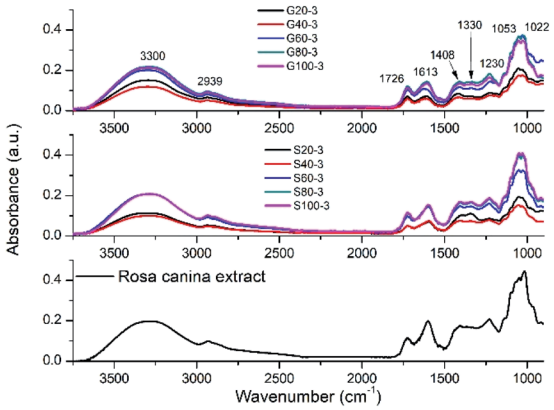

Fig. 5 FTIR spectra of pure *Rosa canina* extract, SNPs and GNPs synthesized with different extract dilutions.

obtained as published earlier.[27,29,31] The broad peak at 3300 cm^{-1} represents the stretching vibrations of O–H bonds. The adsorption band at 2939 cm^{-1} can be attributed to aliphatic C–H bonds.[31] The bands located in 1726, 1613 and 1408 cm^{-1} are corresponding to the symmetric carbonyl group (C═O) stretching vibrations in ketones, aldehydes and carboxylic acids, C═C stretching vibrations from aromatic ring, and C–OH stretching vibrations,[27] respectively. The peaks from 1330 to 1022 cm^{-1} represent the C–O stretching mode of esters.[31] The IR data confirmed the presence of phenolic compounds in the plant extract.

Generally, the antioxidant properties of *Rosa canina* fruits are attributed to ascorbic acid, which is a well-known antioxidant. However, the ascorbic acid content is lower in dry rose hips than fresh forms. Many publications confirmed the high antioxidant capacity and high phenolic compounds of dry *Rosa canina* infusions. Daels-Rakotoarison *et al.* confirmed that the antioxidant properties of rose hips are not due only to ascorbic acid, but also polyphenolics. Phytochemical results showed the presence of proanthocyanidins, flavonoids,[25] ellagic acid, catechin, gallic acid and caffeic acid as major compounds.[44,45]

Ascorbic acid and the phenolic compounds could be participating in the silver and gold nanoparticles formation. It is impossible to describe an exact reaction, but generally, it can be said that hydroxy functional groups containing compounds can reduce metallic cations while forming to ketone groups as R. Kumar published earlier.[42] Hydroxyl compounds also act as stabilizing agents of metallic nanoparticles.[42]

Table 2 summarizes the results obtained in the Z-potential measurements performed for the GNPs and SNPs synthesized at 1×10^{-3} M. The data for both types of NPs indicates that the use of *Rosa canina* extract allowed the formation of negatively charged GNPs and SNPs with Z-potentials varying around −24 mV, which corresponds to stable NPs without been strongly anionic.[46]

Table 2 The Z-potentials for the GNPs and SNPs prepared at 1×10^{-3} M ($HAuCl_4$ or $AgNO_3$, respectively) measured 5 days after the synthesis

Sample	Z-Potential (mV)	Sample	Z-Potential
G20-3	−22.4	S20-3	−29.2
G40-3	−22.4	S40-3	−26.5
G60-3	−24.9	S60-3	−23.6
G80-3	−21.7	S80-3	−24.4
G100-3	−22.0	S100-3	−24.4

Applications of GNPs and SNPs

Since the GNPs and SNPs showed good colloidal stability and low size dispersity, we wanted to explore some practical application where these noble metal colloids could be used. Among these applications, the reduction of 4-nitrophenol (4-NP) to 4-aminophenol (4-AP) using gold nanoparticles as catalysts has become one of the significant model reactions. GNPs can catalyse the reduction of nitro compounds by the electron transfer from donor BH_4^- to acceptor nitro groups.[47–49] The reduction process is followed by measuring absorbance change at 400 nm as a function of time. In a standard quartz cuvette 0.1 mL of 4-NP (4 mM) was mixed with 2.4 mL of water and 0.5 mL of $NaBH_4$ (1 mM); the absorbance spectra were recorded for 20 minutes and no spectral changes were detected (Fig. 6 top). After the addition of 0.1 mL of sample G100-3, the 400 nm spectral band associated to the 4-NP diminished in intensity, while a new band at 300 nm started to appear, indicating the formation of 4-AP (Fig. 6 central panel). The lower panel of Fig. 6 shows that there was a good linear correlation between $\ln(A_t/A_0)$ and the time of reaction ($R^2 = 0.98$), suggesting a pseudo-first-

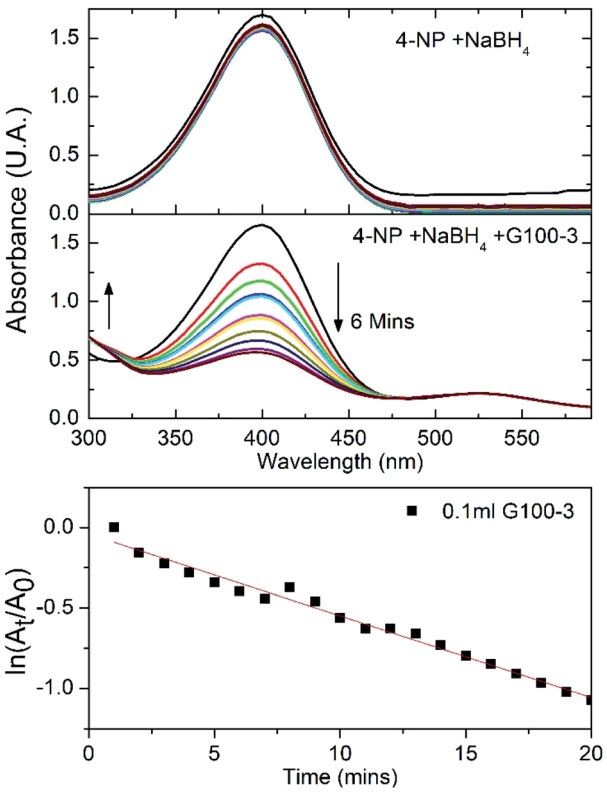

Fig. 6 UV-Vis absorbance spectral kinetics of 4NP + $NaBH_4$ (top panel) and 4NP + $NaBH_4$ + G100-3 (center). The variation of $\ln(A_t/A_0)$ *versus* time, where A_t is the absorbance at 400 nm at a given time and A_0 is the absorbance value t time $t = 0$ min.

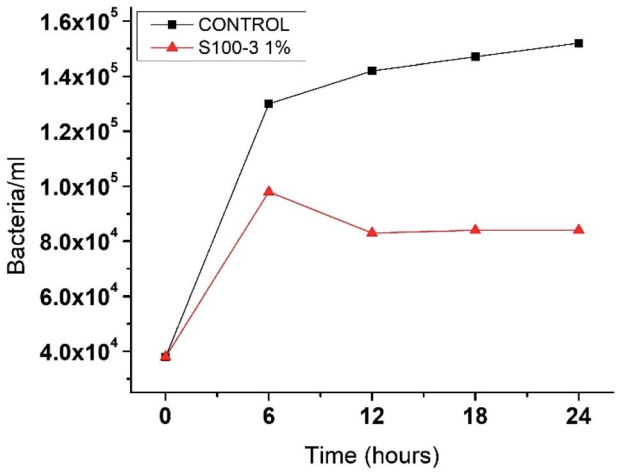

Fig. 7 The kinetic grow of *Escherichia coli*. Control sample and the one supplemented with 0.5 ppm in a 24 hour period.

order kinetics. The rate constant was calculated from the slope of the linear kinetic fitting. The obtained value (5.08×10^{-2} min^{-1}) is comparable to those published earlier.[50,51] With this result we consider that the GNPs we synthesized could be used for catalysis applications.

On the other hand, antimicrobial properties of silver nanoparticles are well-known since Aymonier *et al.* published the synthesis of silver nanoparticles with highly branched amphiphilic polyethyleneimine to get a highly effective and environmentally friendly antimicrobial surface coatings.[52]

To evaluate the antimicrobial properties of the SNPs, *Escherichia coli* was growth in Luria–Bertani medium at 37 °C for 12 hours. Next, 100 μL of the initial inoculum was transferred to 19.9 mL of LB medium supplemented with 1% (v/v) SNPs of samples S100-3, resulting in 0.5 ppm dose. A control sample with no SNPs added was also prepared. This *E. coli* cultures were allowed to growth for 24 hours at 37 °C and the cell count was done every 6 hours by using a 40× microscope objective and a Neubauer chamber. Our result show that for the control there was a fast growing that reached 1.5×10^5 bacteria per mL at 24 hours (Fig. 7), while for the sample supplemented with S100-3 at 0.5 ppm there was a growth up to 1×10^5 bacteria per mL at the 6 hours count, but at the 12 hour count the bacteria diminished to 8.3×10^4 bacteria per mL where it remained constant until the 24 hours passed, indicating that this 0.5 ppm is the SNPs inhibitory concentration of *E. coli*, which is two orders of magnitude lower than the previously reported concentrations by Kumar *et al.*[42]

Conclusions

Gold and silver nanoparticles were successfully produced by a green method using aqueous extract from *Rosa canina* L., which acted as both reducing and stabilizing agent and no other chemical reagent for the stabilization of nanoparticles was required. The developed synthesis method is simple, fast, and environmentally friendly since there were no waste of chemical by-products and it was carried at room temperature. UV-vis spectroscopy and TEM measurements confirmed the presence of quasi-spherical nanoparticles with diameters of approximately 26 for the gold NPs and 34 nm for the silver NPs. XRD showed FCC crystalline structure for both GNPs and SNPs. The effect of extract and noble metal precursor concentrations on particle formation and stability was also studied. The catalytic properties of the GNPs and the antimicrobial effect of the SNPs were also demonstrated.

Author contributions

Pablo Eduardo Cardoso-Avila: investigation, data curation, writing-original draft, visualization, funding acquisition, writing – review & editing; Rita Patakfalvi: conceptualization, methodology, investigation, supervision, resources, writing-original draft, funding acquisition, writing – review & editing; Carlos Rodríguez-Pedroza: methodology, investigation, data curation, visualization; Xochitl Aparicio-Fernández: methodology, investigation; Sofía Loza-Cornejo: methodology, investigation; Virginia Villa-Cruz: methodology, investigation; Evelia Martínez-Cano: methodology, investigation.

Conflicts of interest

There are no conflicts to declare.

Acknowledgements

The authors are grateful to Dr Héctor Gabriel Silva Pereyra (LINAN-IPICyT) for helping in TEM characterization, Christian Albor (CIO) for help in SEM, FT-IR and XRD measurements, and GPOM at CIO for the access to the Z-potential equipment. This research was supported by institutional funds from the Universidad de Guadalajara and Centro de Investigaciones en Óptica A. C., and by CONACyT postdoctoral grant 740141.

References

1 Z. Zhang and P.-C. Lin, Chapter 7 – Noble metal nanoparticles: synthesis, and biomedical implementations, in *Emerging Applications of Nanoparticles and Architecture Nanostructures*, 2018, pp. 177–233, DOI: 10.1016/B978-0-323-51254-1.00007-5.

2 P. Zhao, N. Li and D. Astruc, State of the art in gold nanoparticle synthesis, *Coord. Chem. Rev.*, 2013, **257**, 638, DOI: 10.1016/j.ccr.2012.09.002.

3 X.-F. Zhang, Z.-G. Liu, W. Shen and S. Gurunathan, Silver Nanoparticles: Synthesis, Characterization, Properties, Applications, and Therapeutic Approaches, *Int. J. Mol. Sci.*, 2016, **17**, 1534, DOI: 10.3390/ijms17091534.

4 A. Haider and I.-K. Kang, Preparation of Silver Nanoparticles and Their Industrial and Biomedical Applications: A Comprehensive Review, *Adv. Mater. Sci. Eng.*, 2015, **2015**, 165257, DOI: 10.1155/2015/165257.

5 M. C. Daniel and D. Astruc, Gold Nanoparticles: Assembly, Supramolecular Chemistry, Quantum-Size-Related

Properties, and Applications toward Biology, Catalysis, and Nanotechnology, *Chem. Rev.*, 2004, **104**, 293, DOI: 10.1021/cr030698.

6 P. D. Howes, S. Rana and M. M. Stevens, Plasmonic nanomaterials for biodiagnostics, *Chem. Soc. Rev.*, 2014, **43**, 3835, DOI: 10.1039/c3cs60346f.

7 E. C. Dreaden, A. M. Alkilany, X. Huang, C. J. Murphy and M. A. El-Sayed, The golden age: gold nanoparticles for biomedicine, *Chem. Soc. Rev.*, 2012, **41**, 2740, DOI: 10.1039/c1cs15237h.

8 F. Lu, T. L. Doane, J. J. Zhu and C. Burda, Gold nanoparticles for diagnostic sensing and therapy, *Inorg. Chim. Acta*, 2012, **393**, 142, DOI: 10.1016/j.ica.2012.05.038.

9 J. Turkevich, P. Stevenson and J. Hillier, A study of the nucleation and growth processes in the synthesis of colloidal gold, *Discuss. Faraday Soc.*, 1951, **11**, 55.

10 R. K. Das, V. L. Pachapur, L. Lonappan, *et al.*, Biological synthesis of metallic nanoparticles: plants, animals and microbial aspects, *Nanotechnol. Environ. Eng.*, 2017, **2**, 18, DOI: 10.1007/s41204-017-0029-4.

11 J. Singh, T. Dutta, K. Kim, *et al.*, 'Green' synthesis of metals and their oxide nanoparticles: applications for environmental remediation, *J. Nanobiotechnol.*, 2018, **16**, 84, DOI: 10.1186/s12951-018-0408-4.

12 N. Tarannum, Divya and Y. K. Gautam, Facile green synthesis and applications of silver nanoparticles: a state-of-the-art review, *RSC Adv.*, 2019, **9**, 34926, DOI: 10.1039/c9ra04164h.

13 N. A. I. M. Ishak, S. K. Kamarudin and S. N. Timmiati, Green synthesis of metal and metal oxide nanoparticles via plant extracts: an overview, *Mater. Res. Express*, 2019, **6**, 112004, DOI: 10.1088/2053-1591/ab4458.

14 H. R. El-Seedi, R. M. El-Shabasy, S. A. M. Khalifa, *et al.*, Metal nanoparticles fabricated by green chemistry using natural extracts: biosynthesis, mechanisms, and applications, *RSC Adv.*, 2019, **9**, 24539, DOI: 10.1039/c9ra02225b.

15 N. Tepale, V. V. A. Fernández-Escamilla, C. Carreon-Alvarez, *et al.*, Nanoengineering of Gold Nanoparticles: Green Synthesis, Characterization, and Applications, *Crystals*, 2019, **9**, 612, DOI: 10.3390/cryst9120612.

16 P. Das and V. S. Karankar, New avenues of controlling microbial infections through anti-microbial and anti-biofilm potentials of green mono- and multi-metallic nanoparticles: A review, *J. Microbiol. Methods*, 2019, **167**, 105766, DOI: 10.1016/j.mimet.2019.105766.

17 R. C. Fierascu, A. Ortan, S. M. Avramescu and I. Fierascu, Phyto-Nanocatalysts: Green Synthesis, Characterization, and Applications, *Molecules*, 2019, **24**, 3418, DOI: 10.3390/molecules24193418.

18 K. Kalimuthu, B. S. Cha, S. Kim and K. S. Park, Eco-friendly synthesis and biomedical applications of gold nanoparticles: A review, *Microchem. J.*, 2020, **152**, 104296, DOI: 10.1016/j.microc.2019.104296.

19 M. Scampicchio, J. Wang, A. J. Blasco, A. Sanchez Arribas, S. Mannino and A. Escarpa, Nanoparticle-Based Assays of Antioxidant Activity, *Anal. Chem.*, 2006, **78**, 2060, DOI: 10.1021/ac052007a.

20 J. Wang, N. Zhou, Z. Zhu, J. Huang and G. Li, Detection of flavonoids and assay for their antioxidant activity based on enlargement of gold nanoparticles, *Anal. Bioanal. Chem.*, 2007, **388**, 1199, DOI: 10.1007/s00216-007-1295-y.

21 N. Roy, R. A. Laskar, I. Sk, D. Kumari, T. Ghosh and N. A. Begum, A detailed study on the antioxidant activity of the stem bark of *Dalbergia sissoo* Roxb., an Indian medicinal plant, *Food Chem.*, 2011, **126**, 1115, DOI: 10.1016/j.foodchem.2010.11.143.

22 C. Chrubasik, B. D. Roufogalis, U. Müller-Ladner and S. Chrubasik, A Systematic Review on the *Rosa canina* Effect and Efficacy Profiles, *Phytother. Res.*, 2008, **22**, 725, DOI: 10.1002/ptr.2400.

23 L. Barros, A. M. Carvalho and I. C. F. R. Ferreira, Exotic fruits as a source of important phytochemicals: Improving the traditional use of *Rosa canina* fruits in Portugal, *Food Res. Int.*, 2011, **44**, 2233, DOI: 10.1016/j.foodres.2010.10.005.

24 I. Egea, P. Sánchez-Bel, F. Romojaro and M. T. Pretel, Six Edible Wild Fruits as Potential Antioxidant Additives or Nutritional Supplements, *Plant Foods Hum. Nutr.*, 2010, **65**, 121, DOI: 10.1007/s11130-010-0159-3.

25 D. A. Daels-Rakotoarison, B. Gressier, F. Trotin, C. Brunet, M. Luyckx, T. Dine, F. Bailleul, M. Cazin and J. C. Cazin, Effects of *Rosa canina* Fruit Extract on Neutrophil Respiratory Burst, *Phytother. Res.*, 2002, **16**, 157, DOI: 10.1002/ptr.985.

26 E. M. Wenzig, U. Widowitz, O. Kunert, S. Chrubasik, F. Bucar, E. Knauder and R. Bauer, Phytochemical composition and in vitro pharmacological activity of two rose hip (*Rosa canina* L.) preparations, *Phytomedicine*, 2008, **15**, 826, DOI: 10.1016/j.phymed.2008.06.012.

27 H. Veisi, A. Rashtiani and V. Barjasteh, Biosynthesis of palladium nanoparticles using *Rosa canina* fruit extract and their use as a heterogeneous and recyclable catalyst for Suzuki–Miyaura coupling reactions in water, *Appl. Organomet. Chem.*, 2016, **30**, 231–235, DOI: 10.1002/aoc.3421.

28 J. Pulit and M. Banach, Preparation of Nanosilver and Nanogold Based on Dog Rose Aqueous Extract, *Bioinorg. Chem. Appl.*, 2014, **2014**, 658935, DOI: 10.1155/2014/658935.

29 P. Khademi-Azandehi, J. Moghaddam, R. Khademi-Azandehi, S. S. Veradi-Esfahani and E. Shahabi-Satlsar, Creating Anti-HIV-Infection effect by Synthesis of AuNPs from *Rosa canina* L. Fruit Extract, *J. Nanomed. Res.*, 2017, **6**(3), 00159, DOI: 10.15406/jnmr.2017.06.00159.

30 F. Gulbagca, S. Ozdemir, M. Gulcan and F. Sen, Synthesis and characterization of *Rosa canina*-mediated biogenic silver nanoparticles for anti-oxidant, antibacterial, antifungal, and DNA cleavage activities, *Heliyon*, 2019, **5**, e02980, DOI: 10.1016/j.heliyon.2019.e02980.

31 S. Jafarirad, M. Mehrabi, B. Divband and M. Kosari-Nasab, Biofabrication of zinc oxide nanoparticles using fruit extract of *Rosa canina* and their toxic potential against bacteria: A mechanistic approach, *Mater. Sci. Eng., C*, 2016, **59**, 296–302, DOI: 10.1016/j.msec.2015.09.089.

32 S. Hemmati, L. Mehrazin, M. Hekmati, M. Izadi and H. Veisi, Biosynthesis of CuO nanoparticles using *Rosa canina* fruit

extract as a recyclable and heterogeneous nanocatalyst for C–N Ullmann coupling reactions, *Mater. Chem. Phys.*, 2018, **214**, 527–532, DOI: 10.1016/j.matchemphys.2018.04.114.

33 S. Hemmati, L. Mehrazin, H. Ghorban, S. H. Garakani, T. H. Mobaraki, P. Mohammadia and H. Veisi, Green synthesis of Pd nanoparticles supported on reduced graphene oxide, using the extract of *Rosa canina* fruit, and their use as recyclable and heterogeneous nanocatalysts for the degradation of dye pollutants in water, *RSC Adv.*, 2018, **8**, 21020, DOI: 10.1039/c8ra03404d.

34 S. Hemmati, A. Sedrpoushan, N. Soudalizadeh, K. Khosravi and M. Hekmati, Application of biosynthesized palladium nanoparticles (Pd NPs) on *Rosa canina* fruit extract-modified graphene oxide as heterogeneous nanocatalyst for cyanation of aryl halides, *Appl. Organomet. Chem.*, 2019, **33**, e5103, DOI: 10.1002/aoc.5103.

35 M. D. Méndez-Robles, H. H. Permady, M. E. Jaramillo-Flores, E. C. Lugo-Cervantes, A. Cardador-Martínez, A. A. Canales-Aguirre, F. López-Dellamary, C. M. Cerda-García-Rojas and J. Tamariz, C-26 and C-30 Apocarotenoids from Seeds of *Ditaxis heterantha* with Antioxidant Activity and Protection against DNA Oxidative Damage, *J. Nat. Prod.*, 2006, **69**, 1140, DOI: 10.1021/np050489f.

36 S. Burda and W. Oleszek, Antioxidant and Antiradical Activities of Flavonoids, *J. Agric. Food Chem.*, 2001, **49**, 2774, DOI: 10.1021/jf001413m.

37 Y. Zhou, W. Lin, J. Huang, W. Wang, Y. Gao, L. Lin, Q. Li, L. Lin and M. Du, Biosynthesis of Gold Nanoparticles by Foliar Broths: Roles of Biocompounds and Other Attributes of the Extracts, *Nanoscale Res. Lett.*, 2010, **5**, 1351, DOI: 10.1007/s11671-010-9652-8.

38 S. Link and M. A. El-Sayed, Shape and size dependence of radiative, non-radiative and photothermal properties of gold nanocrystals, *Int. Rev. Phys. Chem.*, 2000, **19**, 409, DOI: 10.1080/01442350050034180.

39 T. Hendel, M. Wuithschick, F. Kettemann, A. Birnbaum, K. Rademann and J. Polte, In Situ Determination of Colloidal Gold Concentrations with UV-Vis Spectroscopy: Limitations and Perspectives, *Anal. Chem.*, 2014, **86**, 11115–11124, DOI: 10.1021/ac502053s.

40 L. M. Liz-Marzán, Tailoring Surface Plasmons through the Morphology and Assembly of Metal Nanoparticles, *Langmuir*, 2006, **22**, 32, DOI: 10.1021/la0513353.

41 M. M. Byranvand and A. N. Kharat, One pot green synthesis of gold nanowires using pomegranate juice, *Mater. Lett.*, 2014, **134**, 64, DOI: 10.1016/j.matlet.2014.07.046.

42 R. Kumar, S. M. Roopan, A. Prabhakarn, V. G. Khanna and S. Chakroborty, Agricultural waste *Annona squamosa* peel extract: Biosynthesis of silver nanoparticles, *Spectrochim. Acta, Part A*, 2012, **90**, 173–176, DOI: 10.1016/j.saa.2012.01.029.

43 D. A. Kumar, V. Palanichamy and S. M. Roopan, Green synthesis of silver nanoparticles using *Alternanthera dentata* leaf extract at room temperature and their antimicrobial activity, *Spectrochim. Acta, Part A*, 2014, **127**, 168–171, DOI: 10.1016/j.saa.2014.02.058.

44 M. K. Hrnčič, D. Cör, P. Kotnik and Ž. Knez, Extracts of White and Red Grape Skin and Rosehip Fruit: Phenolic Compounds and their Antioxidative Activity, *Acta Chim. Slov.*, 2019, **66**, 751–761, DOI: 10.17344/acsi.2019.5253.

45 M. M. Bratu, S. Birghila, A. Popescu, B. S. Negreanu-Pirjol and T. Negreanu-Pirjol, Correlation of antioxidant activity of dried berry infusions with the polyphenols and selected microelements contents, *Bull. Chem. Soc. Ethiop.*, 2018, **32**(1), 1–12, DOI: 10.4314/bcse.v32i1.1.

46 J. D. Clogston and A. K. Patri, Zeta Potential Measurement, in *Characterization of Nanoparticles Intended for Drug Delivery, Methods in Molecular Biology (Methods and Protocols)*, ed. S. McNeil, Humana Press, 2011, vol. 697, DOI: 10.1007/978-1-60327-198-1_6.

47 S. Ghosh, S. Patil, M. Ahire, *et al.*, *Gnidia glauca* flower extract mediated synthesis of gold nanoparticles and evaluation of its chemocatalytic potential, *J. Nanobiotechnol.*, 2012, **10**, 17, DOI: 10.1186/1477-3155-10-17.

48 A. Gangula, R. Podila, M. Ramakrishna, L. Karanam, C. Janardhana and A. M. Rao, Catalytic Reduction of 4-Nitrophenol using Biogenic Gold and Silver Nanoparticles Derived from *Breynia rhamnoides*, *Langmuir*, 2011, **27**(24), 15268–15274, DOI: 10.1021/la2034559.

49 K. Esumi, R. Isono and T. Yoshimura, Preparation of PAMAM– and PPI–Metal (Silver, Platinum, and Palladium) Nanocomposites and Their Catalytic Activities for Reduction of 4-Nitrophenol, *Langmuir*, 2004, **20**(1), 237–243, DOI: 10.1021/la035440t.

50 Y. S. Seo, E.-Y. Ahn, J. Park, T. Y. Kim, J. E. Hong, K. Kim, Y. Park and Y. Park, Catalytic reduction of 4-nitrophenol with gold nanoparticles synthesized by caffeic acid, *Nanoscale Res. Lett.*, 2017, **12**, 7, DOI: 10.1186/s11671-016-1776-z.

51 B. Ankamwar, V. Kamble, U. K. Sur and C. Santra, Spectrophotometric evaluation of surface morphology dependent catalytic activity of biosynthesized silver and gold nanoparticles using UV-vis spectra: A comparative kinetic study, *Appl. Surf. Sci.*, 2016, **366**, 275–283, DOI: 10.1016/j.apsusc.2016.01.093.

52 C. Aymonier, U. Schlotterbeck, L. Antonietti, P. Zacharias, R. Thomann, J. C. Tiller and S. Mecking, Hybrids of silver nanoparticles with amphiphilic hyperbranched macromolecules exhibiting antimicrobial properties, *Chem. Commun.*, 2002, 3018–3019.